MINISTRY OF EDUCATION
SCIENCE AND TRAINING

VIETNAM ACDEMIC OF
AND TECHNOLOGY

GRADUATE UNIVERSITY OF SIENCE AND TECHNOLOGY

Nguyen Thi Van Anh

STUDY ON SYNTHESIS OF FERRATE (FeO_4^{2-}) SOLUTION BY ELECTROCHEMICAL METHOD AND APLICATION FOR WASTWATER TREATMENT

SUMMARY OF DISSERTATION ON SCIENCES OF MATTER

Major: Theoretical and physical chemistry

Code: 9.44.01.19

Hanoi - 2025

The dissertation is completed at: Graduate University of Science and Technology, Vietnam Academy of Science and Technology

Supervisor 1: Dr. Mai Thi Thanh Thuy
Supervisor 2: Prof.Dr. Phan Thi Binh

Reviewer 1: Prof.Dr. Nguyen Xuan Hoan
Reviewer 2: Prof.Dr. Dang Tuyet Phuong
Reviewer 3: Prof.Dr. Mai Xuan Dung

The dissertation is examined by Examination Board of Graduate University of Science and Technology, Vietnam Academy of Science and Technology at 2:30 pm on October 24, 2025.

The dissertation can be found at:
- Library of Graduate University of Science and Technology
- National Library of Vietnam

INTRODUCTION

The rapid growth of the textile industry places a heavy burden on the environment due to the large volumes of wastewater discharged into natural water bodies. According to a report by the World Bank, textile industry effluents account for approximately 20% of global industrial wastewater. This wastewater contains hazardous organic dyes that severely disrupt aquatic ecosystems and pose serious health risks to humans. High concentrations of dyes in water sources reduce light penetration, impairing photosynthesis in aquatic plants and adversely affecting their growth and survival. Moreover, exposure to dye-contaminated water can lead to various health issues, including skin diseases, respiratory problems, and gastrointestinal disorders.

Azo dyes, which contain one or more stable azo groups (–N=N–), account for up to two-thirds of all synthetic dyes and are widely used in the textile, leather, and paper industries. The removal of azo dyes from wastewater has become an urgent challenge, attracting the attention of the scientific community and environmental protection organizations worldwide. Various methods have been applied to treat dye-contaminated wastewater, including Fenton and modified Fenton reactions, electrochemical processes, coagulation, biological treatments, adsorption, and photocatalysis. However, these methods often suffer from limitations such as the generation of secondary pollutants, long treatment times, or complicated material synthesis processes. Recently, ferrate(VI) oxidation has gained significant attention for the treatment of organic dyes due to its advantageous properties. Ferrate(VI) is a strong oxidizing agent with a redox potential as high as 2.2 V in acidic media, enabling it to efficiently degrade a wide range of toxic chemicals within a short time. Compared to other oxidants such as ozone, sodium hypochlorite (NaClO), and Fenton's reagent, ferrate has demonstrated superior treatment efficiency. Moreover, ferrate is regarded as a green oxidant because its reduction product, $Fe(OH)_3$, is an environmentally friendly coagulant. Therefore, ferrate serves multiple roles in wastewater treatment, including acting as an oxidant, disinfectant, decolorizing agent, and coagulant.

There have been three primary techniques for synthesizing ferrate: electrochemical synthesis, thermal synthesis, and wet chemical synthesis. By comparing and evaluating the advantages and disadvantages of various ferrate synthesis methods, several limitations of the wet chemical method

and the thermal method are clear. The wet chemical method has low efficiency and produces many by-products, necessitating an additional purification step to remove excess products after synthesis. The thermal method has low reaction efficiency, is performed at high temperatures posing a risk of fire and explosion, and consumes a lot of energy. Meanwhile, the electrochemical method has recently emerged as a simple method that does not use chemicals and has no toxic by-products, a short synthesis time, and low cost. In addition, the electrochemical method can be used to synthesize ferrate in-situ for direct treatment of polluted wastewater sources, thereby addressing the instability of ferrate and difficulties in storage and transportation.

Therefore, the topic "*Study on the synthesis of ferrate solution (FeO_4^{2-}) by electrochemical method and its application for wastewater treatment*" is proposed.

Research objectives of the dissertation

- To determine the optimal conditions for ferrate synthesis using the electrochemical method.
- To determine the stability of ferrate.
- To apply the synthesized ferrate in the treatment of azo dyes.

Research content of the dissertation

- Study on the conditions affecting the process of ferrate synthesis by electrochemical method including: anode material, electrolyte, electrolysis time, current density, temperature.
- Study on the formation of a passive layer on the anode surface: Study the electrochemical properties, composition, structure, and morphological characteristics of the passive layer formed on the anode surface and the influence of the passive layer on the ferrate synthesis efficiency.
- Study on the factors affecting the stability and kinetics of the ferrate decomposition process.
- Study on the treatment of azo dyes with ferrate solution: study the factors affecting the removal efficiency (treatment time, molar ratio of ferrate/dye, temperature, inorganic ions).

CHAPTER 1. OVERVIEW

1.1. Background of ferrate

Ferrate(VI) is a compound of iron in which iron has an oxidation state of +6. The reduction potential of Fe(VI)/Fe(III) is up to 2.2 V in an acidic environment, so ferrate(VI) has a very strong oxidizing property and can decompose many toxic organic and inorganic substances in water sources. Therefore, ferrate(VI) has high potential in solving environmental problems. Ferrate is quite stable in the solid state, but in an aqueous environment, ferrate is unstable and easily decomposes into iron(III).

There are three methods in the synthesis of ferrate(VI) including: thermal method, wet method, and electrochemical method. In which the electrochemical method is used in many studies because it is a simple method, does not use chemicals and does not have toxic by-products, low cost... In addition, the electrochemical method can be used to synthesize ferrate in-situ to directly treat polluted wastewater sources.

1.2. Application of ferrate

Ferrate is a versatile oxidizing agent, playing many roles in wastewater treatment processes including oxidizing, disinfecting, and coagulating. Ferrate (FeO_4^{2-}) is a very strong oxidizing agent, so it is highly effective in treating toxic organic and inorganic substances in many water sources. The product of the ferrate reduction process is iron(III) hydroxide, an environmentally friendly coagulant capable of removing suspended solids and pollutants such as arsenic(V), cadmium(II), and copper(II). In addition, it is also an effective disinfectant, capable of eliminating pathogenic microorganisms such as viruses, bacteria, and fungi. Thanks to these outstanding advantages, ferrate has been extensively studied in the field of water and wastewater treatment.

1.3. Research background in worldwide and Vietnam

Currently, many research groups around the world have focused on synthesizing ferrate by electrochemical methods, developing on-site ferrate production systems, and applying them in water and wastewater treatment. Additionally, the application of ferrate in treating toxic, difficult-to-decompose organic substances, and chlorine-resistant viruses has also been researched and shown good treatment efficiency. In Vietnam, research on ferrate is still limited, and there has been little or no work on its electrochemical synthesis by domestic research groups.

CHAPTER 2. EXPERIMENT AND RESEACH METHODS

2.1. Experiment

Anode materials

The anode electrodes used for ferrate synthesis via the electrochemical method were fabricated from three materials: CT3 steel (mild steel – MS), grey cast iron (GCI), and ductile iron (DI). These materials were sourced from Hanoi Mechanical Limited Company, Vietnam. The composition of these materials is presented in Table 2.1

Table 2.1. *Composition of anode materials using for ferrate electrochemical synthesis.*

Materials	Mass composition (%)					
	Fe	**C**	**Si**	**P**	**S**	**Mn**
DI	93.701	3.650	2.330	0.010	0.009	0.300
GCI	92.480	5.214	1.778	0.011	0.021	0.496
MS	98.843	0.268	0.265	0.023	0.021	0.580

Ferrate synthesis

Note:
(1)- Electrochemical workstation
(2)- Magnetic stirrer
(3)- Electrolyte
(4)-Ag/AgCl reference electrode
(5)- Anode
(6)- Titanium counter electrode
(7)- Membrane

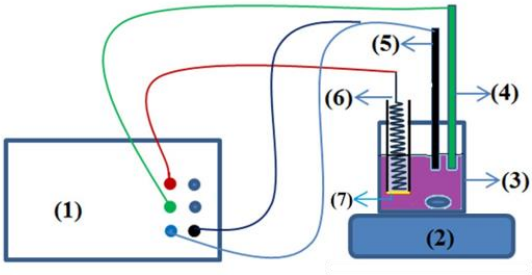

Figure 2.1*. Schematic of the electrochemical cell of ferrate synthesis*

Ferrate was synthesized by electrochemical method using a three-electrode system consisting of an Ag/AgCl reference electrode (saturated KCl), a titanium counter electrode, and working electrodes made from DI, GCI, and MS (Figure 2.1). The experiments were conducted using an IM6 electrochemical workstation (Zahner Elektrik, Germany), with variations in current density ranging from 10 to 50 mA/cm², NaOH electrolyte concentration from 8 to 16 M, and reaction temperature from 10 to 50 °C. The synthesized ferrate solution will be analyzed using UV-Vis spectroscopy to determine its concentration. The electrochemical and physicochemical properties of the anode will be characterized both before and after the synthesis.

Treatment of azo dyes by ferrate

Reactive azo dyes, namely reactive red 195 (RR195) and methyl orange (MO), with an initial concentration of 50 mg/L, were treated using a ferrate(VI) solution at a concentration of 1500 ± 50 mg/L. The dye and ferrate solutions were mixed and stirred continuously at 500 rpm for the first 5 minutes, followed by static conditions for varying durations ranging from 0 to 55 minutes. The effects of pH (ranging from 1 to 9), temperature (10–50 °C), and the molar ratio of ferrate to dye were investigated.

2.2. Research methods

2.2.1. The electrochemical methods

The experiments for electrochemical ferrate synthesis and electrochemical characterization of the anode materials were conducted using an IM6 electrochemical workstation (Zahner Elektrik, Germany). The electrochemical measurements performed included:

- Cyclic Voltammetry (CV)
- Electrochemical Impedance Spectroscopy (EIS)
- Linear Sweep Voltammetry (LSV)

2.2.2. The physicochemical analysis methods

The changes in the surface structure of the anode before and after ferrate synthesis were evaluated using the following physicochemical analysis methods.

- Scanning electron microscopy (SEM) and energy dispersive X-ray spectroscopy (EDS) were performed using a FE SEM Hitachi S-4800 (Japan).
- X-ray diffraction (XRD) was performed on a D8-ADVANCE (Germany)
- Raman spectroscopy was carried out on a LabRAM HR Evolution (HORIBA Scientific, Japan)

2.2.3. Method for analyzing the concentration of ferrate and azo dyes

The concentrations of ferrate and dyes before and after treatment were determined by UV-Vis method on Perkin Elmer UV/Vis spectrometer Lambda 35 (USA) and Hach-DR6000 (USA). The products formed after the decomposition of the dye by ferrate were determined by liquid chromatography-mass spectrometry LC-MS on the X500R, QTOF system (SCIEX, USA).

CHAPTER 3. RESULTS AND DISCUSSION

3.1. Study on ferrate synthesis by electrochemical method

3.1.1. Anode material selection

Study on the electrochemical characteristics of anode materials

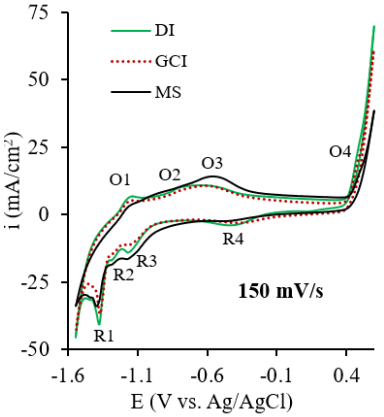

Figure 3.1. *CV curves of DI, GCI, MS in 14 M NaOH solution.*

Figure 3.1 shows the cyclic voltammetry (CV) curves of the anode electrodes in 14 M NaOH solution. The results indicate that there are four oxidation peaks (O1, O2, O3, and O4) and four reduction peaks (R1, R2, R3, and R4). In which the 4 oxidation peaks O1, O2, O3, O4 correspond to each process of changing the oxidation number of iron in the direction of increasing potential as follows: Fe → Fe(II) → Fe_3O_4 → Fe(III) → Fe(VI).

Thus, the oxidation peaks O1, O2, and O3 correspond to the formation of intermediate species (Fe(II), Fe_3O_4, Fe(III)), while the O4 peak is specifically associated with the formation of ferrate (Fe(VI)).

Comparing the CV spectra between three electrodes MS, GCI, DI at the same scanning speed of 150 mV/s shows that the MS anode has the highest peak pair (O3, R3) and the lowest peak pair (O4, R4) while the DI anode has the highest peak pair (O4, R4). This evidence shows that the formation of the passive layer on MS is easier and the formation of ferrate on MS is more difficult than the remaining electrodes. On the contrary, the ability to form ferrate on DI is the easiest.

Figures 3.2a–c show the Bode plots of the anode materials at different temperatures, and Figure 3.2d presents their impedance (Z) values at 10 mHz. As temperature increased from 10 °C to 50 °C, Z values

decreased for all materials: DI from 768 to 164 Ω, GCI from 932 to 173 Ω, and MS from 2350 to 159 Ω, indicating enhanced iron oxidation at higher temperatures. Among them, DI showed the lowest impedance across all temperatures, demonstrating its superior electrochemical performance for ferrate synthesis..

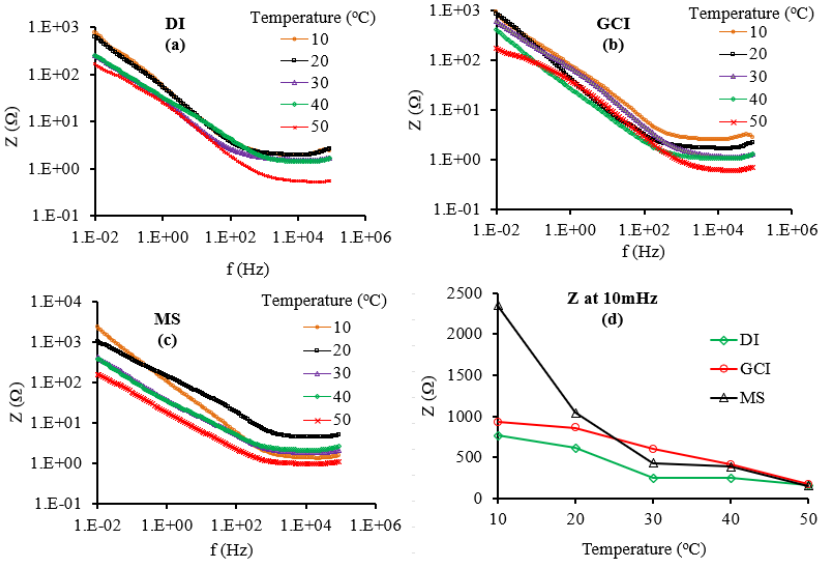

Figure 3.2. *The Bode plots at different temperatures of (a) DI, (b) GCI, (c) MS and (d) Impedance values at 10 mHz.*

Effect of anode material on the ferrate synthesis process

The results in Figure 3.3 demonstrated that ferrate concentration and synthesis yield increased markedly as the temperature rose from 10 °C to 40 °C, followed by a decline when the temperature was increased to 50 °C across all electrode types. Among the tested anodes, DI consistently produced the highest ferrate concentration, while MS yielded the lowest at all temperatures. At 40 °C, the ferrate concentrations achieved were 437 mg/L (DI), 342 mg/L (GCI), and 328 mg/L (MS). The DI anode also exhibited the highest synthesis yield, reaching 74 % at 40 °C. These findings suggest that DI is a promising material for anode fabrication in electrochemical ferrate synthesis systems. The optimal temperature range

for ferrate synthesis using nodular cast iron anodes is between 30 °C and 40 °C.

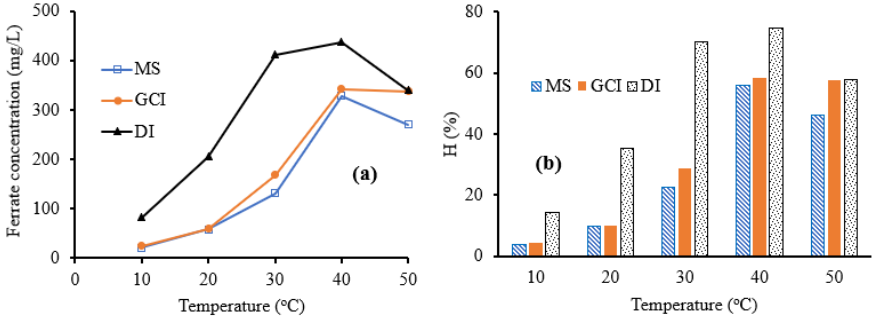

Figure 3.3. *Effect of anode materials on (a) ferrate concentration, and (b) synthesis efficiency*

Study on structural and morphological characteristic of anode materials

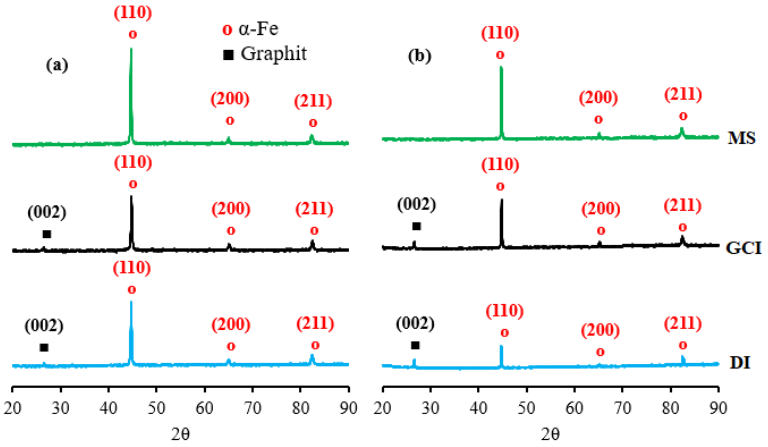

Figure 3.4*. XRD patterns of DI, GCI and MS (a) before and (b) after 180 minutes ferrate electrochemical synthesis.*

Figure 3.4 shows that after 3 hours of electrolysis, the characteristic peaks corresponding to the ferrite structure on all materials significantly decreased. This reduction is attributed to the accumulation of iron oxide and hydroxide products on the anode surface.

SEM images after 3 hours of electrolysis for DI and GCI electrodes (Figures 3.5d and 3.5e) reveal that severe corrosion occurs at the interface between the graphite and ferrite phases. This phenomenon is explained by these interfacial regions having less stable crystal structures, making them more susceptible to electrochemical corrosion. As a result, DI and GCI materials exhibit higher ferrate synthesis efficiency compared to MS.

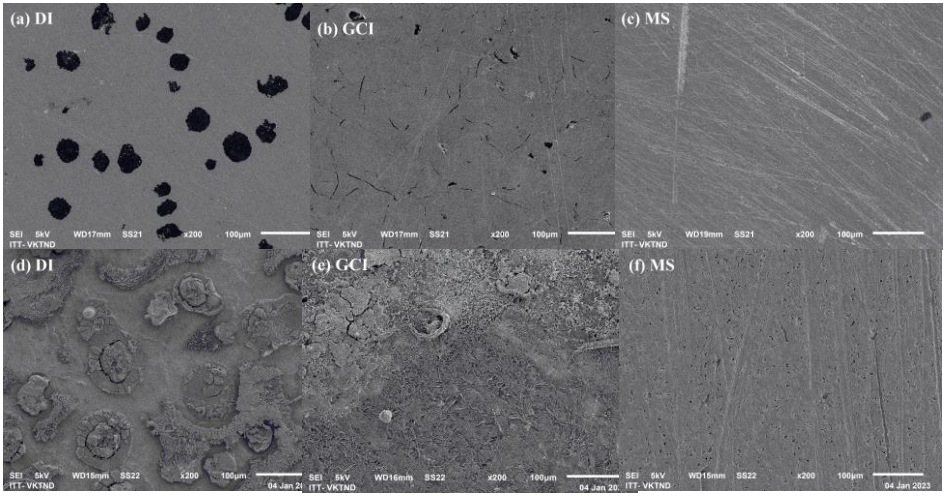

Figure 3.5. *SEM images of anode materials (a,b,c) before, and (d,e,f) after 3 hours ferrate electrochemical synthesis.*

3.1.2. Study on the synthesis conditions of ferrate by electrochemical method using ductile iron anode.

Important variables affecting ferrate concentration and synthesis efficiency in electrochemical ferrate synthesis include electrode surface area-to-volume ratio (S/V), current density, electrolysis time, and electrolyte concentration. To optimize ferrate production using ductile iron anodes, each of these variables was systematically investigated. The resulting performance data are presented in Figures 3.6 and 3.7.

Figure 3.6 shows that increasing the NaOH concentration from 8 to 14 M significantly enhances the ferrate concentration, reaching nearly 200 mg/L at 14 M. However, further increasing the NaOH concentration to 16 M results in a slight decrease in ferrate yield. Therefore, 14 M NaOH is

identified as the optimal electrolyte concentration for electrochemical ferrate synthesis using DI anode.

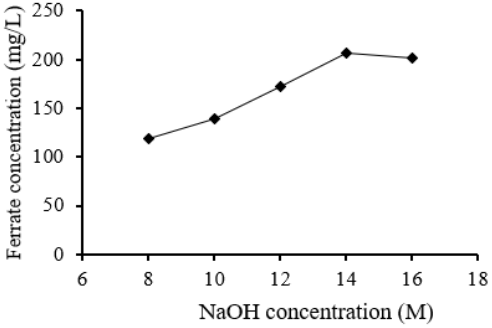

Figure 3.6. *Effect of NaOH concentration on ferrate synthesis process.*

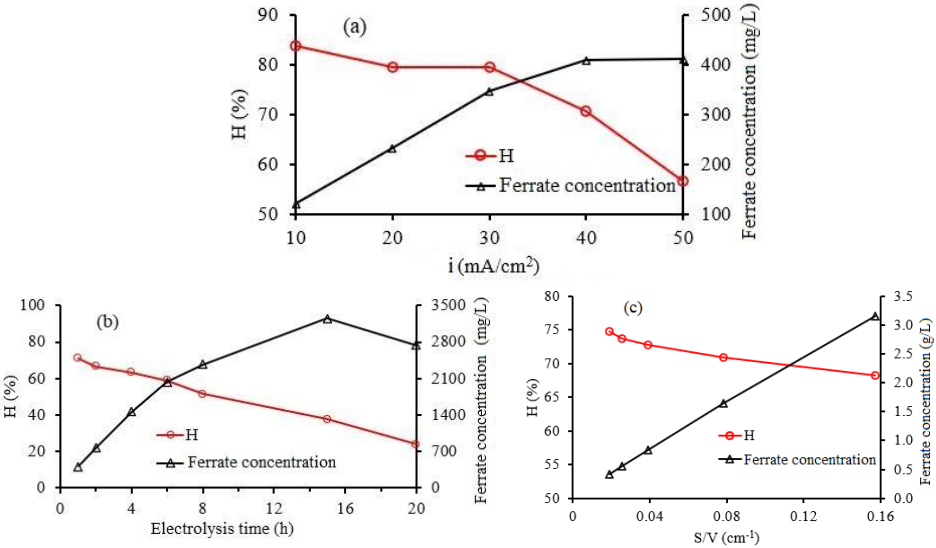

Figure 3.7. *Effect of (a) current density, (b) electrolysis time, (c) S/V ratio on ferrate synthesis process.*

Figure 3.7a shows the effect of current density on the ferrate concentration and synthesis efficiency. Increasing the current density from 10 to 40 mA/cm² resulted in a ferrate concentration increase from 120.45 to 407.87 mg/L, accompanied by a decrease in synthesis efficiency from 83.75 to 70.65 %. Further increasing the current density to 50 mA/cm² caused a slight drop in ferrate concentration and a sharp fall in efficiency to

56.55 %. At high current density, the vigorous oxygen evolution reaction lead to bubble coverage on the anode surface, which restrict interface contact between the electrode and electrolyte. Consequently, 40 mA/cm² was determined as the optimal current density for ferrate synthesis.

Figure 3.7b shows the dependence of ferrate concentration and synthesis efficiency on electrolysis time. The synthesis efficiency decreases with electrolysis time and to ensure the synthesis efficiency is above 60%, the synthesis time must be less than 6 hours.

The S/V ratio is a critical factor influencing the electrochemical ferrate synthesis process. As shown in Figure 3.7c, increasing the S/V ratio from 0.019 to 0.157 cm^{-1} raised the ferrate concentration over sevenfold, whereas the efficiency dropped by approximately 10 %. Despite this minor decrease in efficiency, a higher S/V ratio is advantageous, as it allows the desired ferrate concentration to be achieved in a shorter electrolysis time.

The above results indicate that the optimal conditions for ferrate synthesis using a ductile iron anode are a 14 M NaOH electrolyte solution, a current density of 40 mA/cm², and an electrolysis time of less than 6 hours, S/V ratio of 0,08 cm^{-1}.

3.2. Study on the formation passive layer on the ductile iron anode surface over time.

3.2.1. Study on the structural and morphological changes of the dutile iron anode over time.

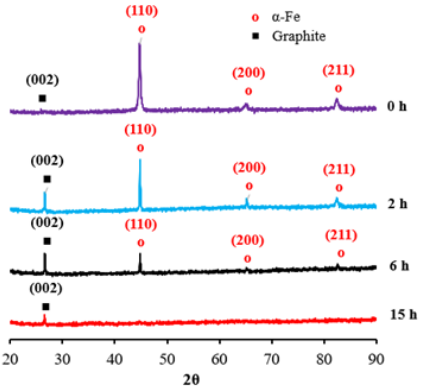

Figure 3.8. *XRD patterns of the DI anodes before and after different electrolysis times.*

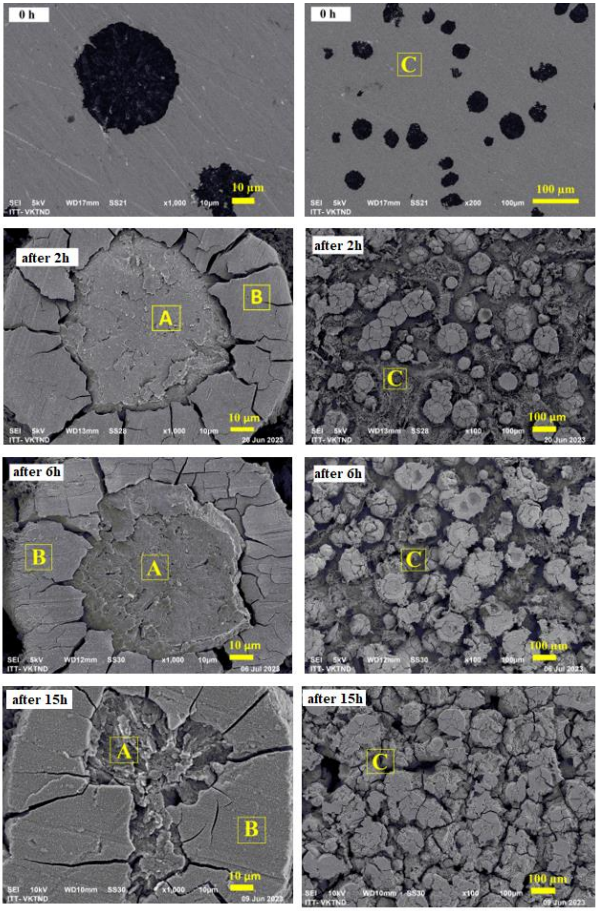

Figure 3.9. *SEM images of the DI anodes before and after different electrolysis times.*

Figure 3.8 shows the XRD patterns of DI anodes before and after electrolysis for 2, 6, and 15 hours. The characteristic diffraction peaks of the ferrite (α-Fe) crystal structure appeared in both samples before and after electrolysis for 2 and 6 hours. However, the intensity of these peaks gradually decreased with increasing electrolysis time and disappeared in the DI sample after 15 hours of electrolysis. This reduction is attributed to the formation of an amorphous iron oxide passivation layer that thickens over time. This phenomenon is demonstrated in the SEM image (Figure 3.9), where a passivation layer completely covers the anode surface after 15 hours of electrolysis.

Figure 3.9 presents the SEM images of the DI anodes before and after electrolysis. Oxidation occurs strongly around the spherical graphite particles, forming a fine-textured passive layer (region B) surrounding the nodules (region A); additionally, the porous passive layer was also formed in the outer area of the graphite nodules (region C). Increasing electrolysis time from 2 to 15 h, the area of region B expanded, whereas regions A and C narrowed.

3.2.2. Study on composition of passive layer

The elemental composition determined by EDS method on the DI anode surface in regions A, B, C at different electrolysis times is summarized in Table 3.2.

After electrolysis time of 2 and 6 hours, region A was mainly composed of carbon (95.2 % and 94.1 %). After 15 hours of electrolysis, carbon composition dropped to 19.7 %, while composition of Fe and O increased, indicating iron oxide formation on the graphite nodules surface.

In region B, the carbon content remains nearly constant at around 10 % across different electrolysis durations. The mass ratio between iron and oxygen varies slightly from 1.9 to 2.1, predicting that the passive layer in region B likely consists of a mixture of FeOOH, Fe_2O_3, and Fe_3O_4.

***Table 3.1**. Mass composition of elements on the DI anodes surface after different electrolysis times.*

Area	Electrolysis time (h)	Mass composition (wt %)				
		Fe	O	C	Si	Na
A	2	1.7	3.1	95.2	-	-
	6	2.1	3.6	94.1	0.2	-
	15	52.3	25.5	19.7	0.2	1.9
B	2	57.5	26.9	10.5	3.0	2.2
	6	54.4	28.6	10.7	3.0	2.3
	15	57.8	27.9	9.6	0.7	3.2
C	2	80.8	11.3	6.1	1.1	0.7
	6	68.1	15.5	12.6	2.0	0.8
	15	59.1	28.6	8.3	0.4	2.8

In region C, the iron component was still dominant after 2 h of electrolysis (80.8 %), and oxygen accounted for 11.2 %, so only a small amount of iron oxide was formed on the surface. The iron component decreased and the oxygen component gradually increased with increasing electrolysis time to 6 and 15 h, indicating that the iron oxide layer on region C thickened over time.

The Raman spectra given in Figure 3.10 show the formation of iron oxides on the surface of DI after 2, 6 and 15 h of electrolysis.

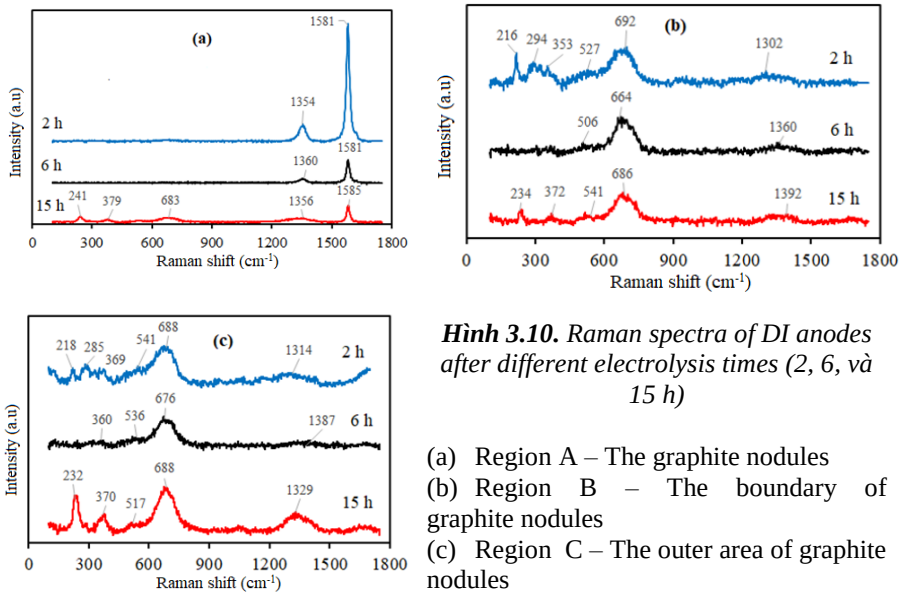

Hình 3.10. *Raman spectra of DI anodes after different electrolysis times (2, 6, và 15 h)*

(a) Region A – The graphite nodules
(b) Region B – The boundary of graphite nodules
(c) Region C – The outer area of graphite nodules

The Raman spectra of Region A show graphite peaks at ~1580 and ~1355 cm^{-1} after 2 and 6 hours of electrolysis. After 15 hours, in addition to the graphite peaks at 1585 and 1356 cm^{-1}, new peaks appear at 241 and 379 cm^{-1} (α-Fe_2O_3) and at 683 cm^{-1} (Fe_3O_4). This suggests that prolonged electrolysis leads to graphite nodules being covered by iron oxides from ferrate decomposition.

The Raman spectra in Figure 3.10c, similar to Figure 3.10b, show that after 2 hours of electrolysis, the regions B, C contained a mixture of α-FeOOH, α-Fe_2O_3, and Fe_3O_4. However, after 6 and 15 hours, only α-Fe_2O_3 and Fe_3O_4 are detected. Notably, the Fe_3O_4 peaks are consistently more

intense than those of α-Fe_2O_3 and FeOOH at all electrolysis durations. This suggests that Fe_3O_4 is the predominant component of the passive layer, which is consistent CV curves analysis (Figure 3.11).

3.2.3. Ảnh hưởng của lớp thụ động tới tính chất điện hóa của anot

CV and EIS spectra were measured at different electrolysis times to evaluate the impact of the passivation layer on the electrochemical properties of the anode. The results are shown in Figures 3.11 and 3.12.

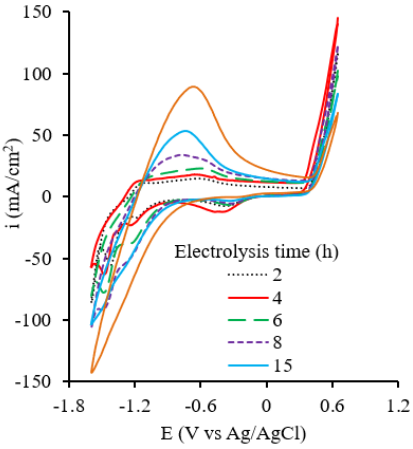

Figure 3.11. *CV curves of DI anode after different electrolysis times.*

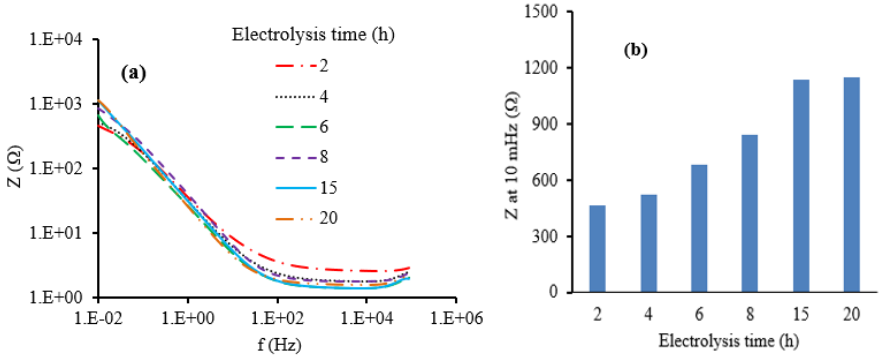

Figure 3.12. *Bode plots of DI anode at different electrolysis times.*

After electrolysis time greater than 6 hours, the CV curves mainly show the O2 peak, O4 peak shoulder and R4 peak. Increasing electrolysis time from 8 to 20 hours raised the height of the O2 peak, but decreased the

hight of O4 peak shoulder and R4 peak. Therefore, with electrolysis time greater than 6 hours, the passivation layer on the DI anode will significantly inhibit the formation of ferrate.

The impedance values at low frequency of 10 mHz increased with rising electrolysis time from 2 to 20 hours because of the developing of the passive layer on the anode surface. This result is consistent with the CV measurement results presented above.

3.2.4. Effect of passive layer on ferrate synthesis process

As shown in Figure 3.13, the ferrate concentration remained relatively stable in the range of 410 to 426 mg/L during the first 1–6 hours of electrolysis. However, it dropped significantly after 8–20 hours, with a 46 % decrease at 20 hours. The optimal operating time of the electrolysis cycle for the DI anode was 6 hours. Therefore, after about 6 hours of operation, the anode needs to be cleaned on the surface to remove the passive layer to ensure that the ferrate synthesis process takes place effectively.

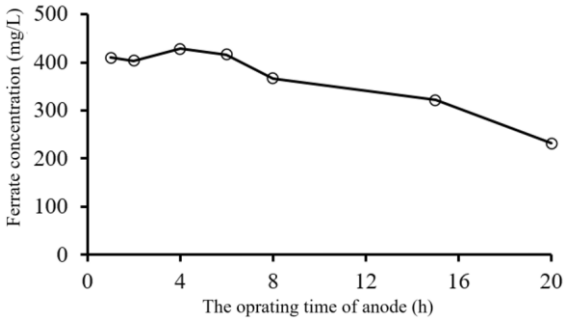

Figure 3.13. *Effect of operating time of anode on ferrate concentration.*

3.3. Study on the stability of synthesized ferrate solutions

3.3.1. Factors affecting the stability

Figure 3.14a illustrates the impact of temperature on ferrate solution stability. The results indicate that ferrate decomposed more rapidly at higher temperatures. At 4 °C, decomposition was minimal, with ferrate concentration remaining nearly constant after 8 hours. In contrast, significantly greater decomposition occurred at 20 °C, 30 °C, and 40 °C.

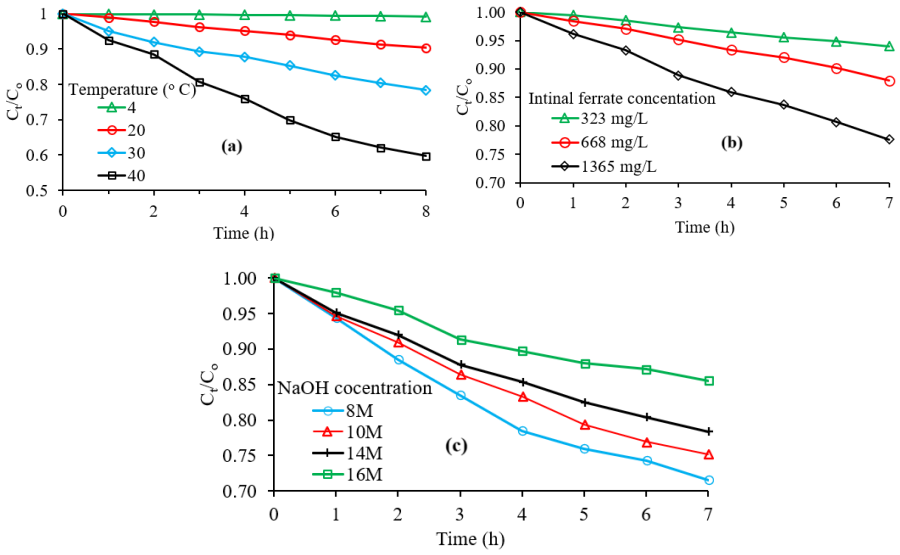

***Figure 3.14**. Effect of (a) temperature, (b) intinal ferrate concentration, and (c) NaOH concentration on the stability of ferrate solution.*

Figure 3.14b shows that the decomposition rate of ferrate depends on its initial concentration, the higher the initial concentration, the faster the decomposition rate. Specifically, after 7 hours, the ferrate of the sample with an initial concentration of 323 mg/L decomposed by about 6 %, while for the sample with an initial concentration of 1365 mg/L, this value increased to nearly 23 %.

Figure 3.14c illustrates the effect of NaOH concentration on ferrate stability. The decomposition rate of ferrate increases as NaOH concentration decreases. After 7 hours, approximately 30 % of ferrate decomposed in 8 M NaOH solution—about twice the amount compared to that in 16 M NaOH.

3.3.2. Kinetics of ferrate solution decomposition

The relationship between $\frac{1}{C_t} - \frac{1}{C_0}$ and t at different temperatures is shown in Figure 3.15. The linear trend observed, with a coefficient of determination R^2 greater than 0.99 at all temperatures, confirms that the ferrate decomposition in 14 M NaOH follows a second-order kinetic model. The slope of each line corresponds to the reaction rate constant, as

summarized in Table 3.2. As temperature increases, the rate constant rises markedly about 16-fold from 4 to 20 °C and nearly 100-fold from 4 to 40 °C.

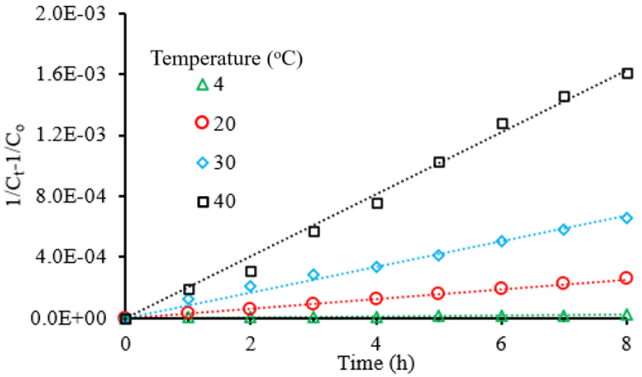

Figure 3.15. *Relationship between* $\frac{1}{C_t} - \frac{1}{C_0}$ *and time.*

Table 3.2. *Rate constants of ferrate decomposition reaction at different temperatures.*

T	k_2		R^2
°C	$(mg/L)^{-1}h^{-1}$	$M^{-1}.s^{-1}$	
4	$2.03x10^{-6}$	$6,77x10^{-5}$	0.9945
20	$3.16x10^{-5}$	$1,05x10^{-3}$	0.9989
30	$8.42x10^{-5}$	$2,81x10^{-3}$	0.9969
40	$2.03x10^{-4}$	$6,77x10^{-3}$	0.9977

3.4 Study on treatment of azo dyes methyl orange(MO) and reactive red 195 (RR195)

3.4.1. Study on optimal conditions for dye treatment

pH is a critical factor in the treatment of azo dyes with ferrate, as it influences both the oxidizing power and the decomposition rate of ferrate. As illustrated in Figure 3.16, the dye removal efficiency is higher under acidic conditions than in alkaline conditions, with optimal performance observed at pH 3. In contrast, temperature has a minimal effect on the dye treatment efficiency, as shown in Figure 3.16b.

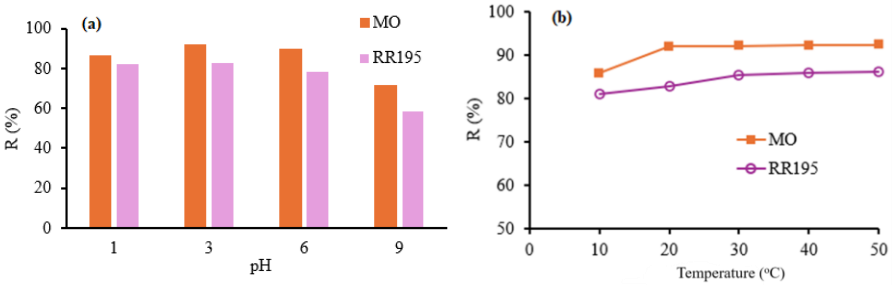

Figure 3.16. *Effect of (a) pH, and (b) temperature on MO and RR195 removal efficiency.*

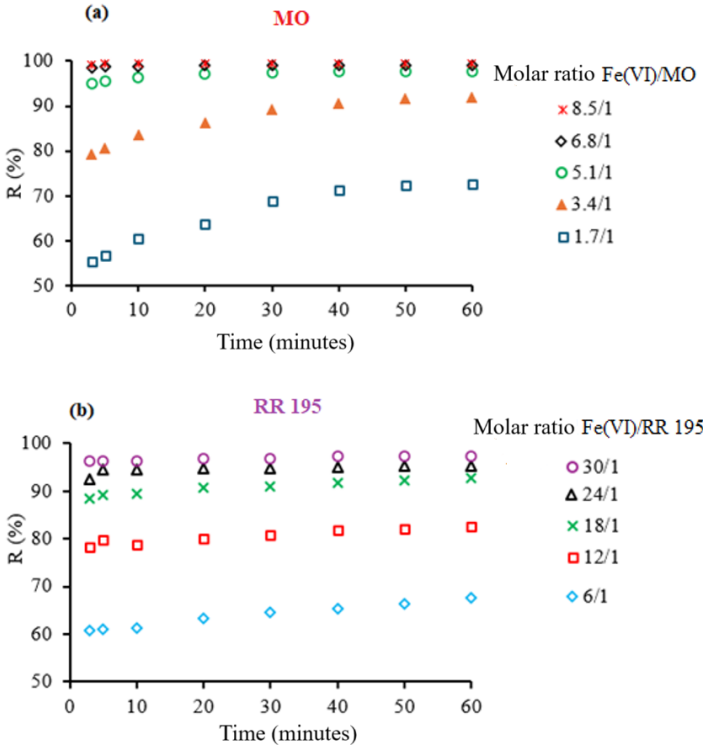

Figure 3.17. *Effect of molar ratio of ferrate/dye on degradation efficiency a) MO, b) RR195.*

Figure 3.17 shows the effect of ferrate/dyes molar ratios on treatment efficiency over time. The oxidation reaction of MO and RR 195 of ferrate

occurs mainly in the first 3-5 minutes. The RR 195 removal efficiency reaches 96 % after 3 minutes at the molar ratio of Fe(VI)/RR 195 = 24/1.0, the MO removal efficiency reaches 99.3 % after 3 minutes at the molar ratio of Fe(VI): MO of 8.5/1.0.

3.4.2. Effect of some inorganic ions on the dye treatment process

In addition to organic dyes, dye wastewater also contains various inorganic ions such as Cu^{2+}, Mg^{2+}, Fe^{3+}, Mn^{2+}, Cl^{-}, NO_3^{-}, CO_3^{2-}, and SO_4^{2-}. Figures 3.18 and 3.19 illustrate the influence of some anions and cations on the dye removal efficiency.

The results indicate that Fe^{3+} and Mg^{2+} ions almost did not affect the dye degradation efficiency, whereas the presence of Cu^{2+} ions leaded to a decrease in treatment performance. In contrast, some anions such as Cl^{-} and NO_3^{-} enhanced the dye removal efficiency

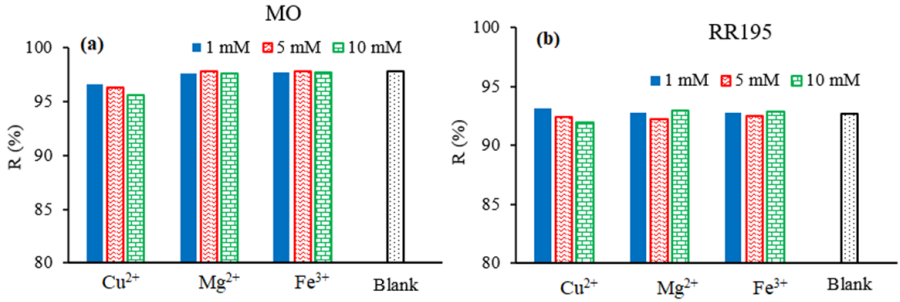

Figure 3.18. *Effect of cations on the degradation efficiency of (a) MO, (b) RR195 by ferrate.*

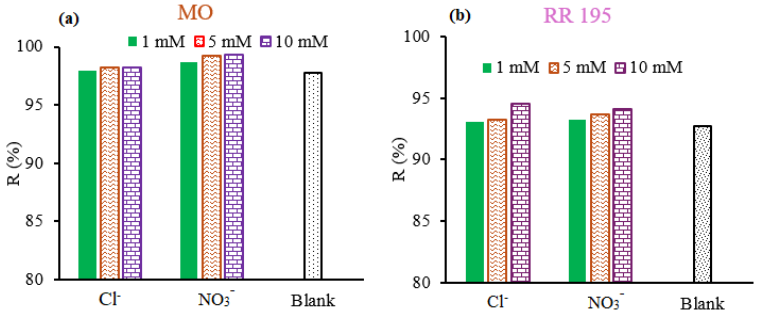

Figure 3.19. *Effect of anions on the degradation efficiency of (a) MO, (b) RR195 by ferrate.*

3.4.3. Cơ chế phân hủy chất màu azo bằng ferrate

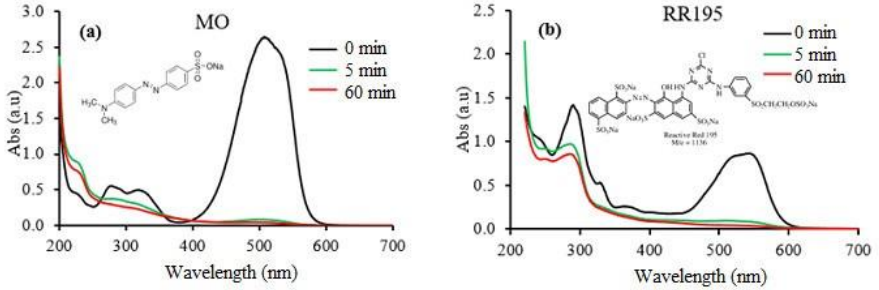

Figure 3.20 *UV-vis spectra of (a) MO, (b) RR195 solutions before and after treatment.*

Figure 3.20 shows the UV–vis spectra of MO and RR195 solutions before and after treatment times of 5 and 60 minutes. Before treatment, both dyes exhibited a strong absorption peak in the visible region at 509 nm (MO) and 545 nm (RR195), corresponding to the azo bond (–N=N–). Additionally, the UV–vis spectrum of MO showed two peaks and that of RR195 showed four peaks in the UV region, attributed to aromatic rings. As the treatment time increased from 5 to 60 minutes, the intensity of all peaks decreased, indicating the breakdown of azo bonds and the destruction of aromatic rings. After 60 minutes of treatment, all absorption peaks became very weak or nearly disappeared, suggesting that most organic intermediates and the dyes MO and RR195 were decomposed and removed.

3.4.3. Comparison of the efficiency of azo dye decomposition by ferrate with other methods.

To remove MO and RR195 from wastewater, many treatment methods have been used, such as adsorption, chemical coagulation, photocatalysis, electrocatalysis, and biological methods. However, adsorption and chemical coagulation transfer dyes from the liquid phase to the solid phase, thereby causing secondary pollution. Biological methods are not suitable for MO treatment due to their low biodegradability. Tables 3.3 and 3.4 compare different methods for MO and RR195 treatment. The results show that ferrate (VI) has better treatment performance in a short time. Moreover, because ferrate is a green oxidant, easy to synthesize, and low cost, ferrate (VI) becomes a viable option for the removal of azo dyes in textile wastewater.

Bảng 3.3. *Comparison of MO treatment methods.*

Method/Material	**Treatment time (mintutes)**	**Removal efficiency (%)**
Oxidation ($O_3/K_2S_2O_8$)	50	98.6
Fenton reaction (H_2O_2/Fe^{2+} - UV)	15	97.8
Photocatalysis $[FemIL@SiO_2@Mag]_2MoO_4$	30	99.0
Photocatalysis (Fe_3O_4/TiO_2)	60	90.3
Photocatalysis (MoS_2/Fe_3O_4)	100	79.5
Electrocatalytic oxidation (PbO_2 -TiO_2)	50	99.3
Electrocatalytic oxidation (Ti/SnO_2 -Sb_2O_3 /PbO_2 -TiO_2)	240	95.5
Adsorption (MOF: Ni-doped ZIF-67)	120	82.9
Photoelectrocatalytic process (Reduced – TiO_2)	30	98.4
Advance oxidation (ferrate(VI))	3 60	99.3 99.4

Bảng 3.4. *Comparison of RR195 treatment methods.*

Method/Material	**Treatment time (minutes)**	**Removal efficiency (%)**
Electrochemical oxidation (graphite electrode)	60	93.9
Electro-Fenton reaction (Fe_3O_4/rGO)	60	93.3
Catalytic ozonation (nZVI-Ca-Alginate Beads)	90	99.0
Electro ozone generation ($Ti/TiHx/SnO_2$-Sb_2O_5-NiO-CNT electrode)	30	96.0
Photocatalysis ($Ag/TiO_2/Fe_3O_4$ nanocomposite)	30	98.0
Adsorption (chitosan-cellulose)	320	97.2
Adsorption (crosslinked oxalic acid/chitosan hydrogels)	600	90.6
Advance oxidation (ferrate(VI))	3 60	96.3 97.3

CONCLUSIONS

1. Ferrate solution was successfully synthesized using galvanostatic technique. Compared to gray cast iron and CT3 steel, the ductile iron material had a substantially greater ferrate synthesis efficiency, reaching 74 % at 40 °C thanks to the porous structure of spherical graphite and high Si content in ductile iron. The optimal parameters for ferrate production using ductile iron anode were: 14 M NaOH electrolyte solution, current density 40 mA/cm^2, temperature 30-40 °C, and S/V ratio 0.08 cm^{-1}.

2. SEM images and XRD patterns confirmed the formation and progressive thickening of a passive layer on the surface of ductile iron anodes during electrochemical ferrate synthesis. CV, Raman and EDS spectra show that the passive layer forms due to the accumulation of Fe_3O_4 on the anode surface and the decomposition of ferrate into Fe_2O_3 that adheres to the anode surface. EIS and CV spectra demonstrate that the passive layer reduces the electrochemical activity of the anode, leading to a decrease in ferrate production efficiency. The optimal operating cycle of the anode is 6 hours; after each cycle, the surface needs to be treated to remove the passive layer.

3. The stability of ferrate solution depends on factors including: temperature, NaOH concentration and initial ferrate concentration. As the temperature and initial ferrate concentration increase, the stability decreases, conversely, as the NaOH concentration increases, the stability increases. Ferrate solution is optimally stored at 4 ^oC and NaOH concentration of 14-16 M.

4. The efficiency of MO and RR195 removal by ferrate depends on pH and the molar ratio of Fe(VI)/azo dye. At the optimal pH of 3, the removal efficiency reached over 90% when the molar ratio of Fe(VI)/MO > 5.1/1 and Fe(VI)/RR195 > 18/1. The dyes decomposition reaction took place mainly in the first 3–5 minutes, with removal efficiency reaching 99.3% for MO (Fe(VI)/MO = 8.5/1.0) and 93% for RR195 (Fe(VI)/RR195 = 24.1/1.0) after 3 minutes.

NEW CONTRIBUTIONS OF THE THESIS

1. This dissertation is the first study to synthesize ferrate by the electrochemical method using a ductile iron anode, achieving a high efficiency of 74% at 40 °C.
2. It elucidates the mechanism of passive film formation on the surface of the ductile iron anode during electrochemical ferrate synthesis. The main component of the passive layer was Fe_3O_4 and the formation of the passive layer reduced the ferrate synthesis efficiency.
3. It demonstrates the effective application of ferrate in treating the azo dye Reactive Red 195, with an Fe(VI)/RR195 molar ratio greater than 18:1, achieving a treatment efficiency of over 96%.

LIST OF THE PUBLISHED PAPERS RELATED TO THE DISSERTATION

1. Thi Thanh Thuy Mai, **Thi Van Anh Nguyen**, Thi Binh Phan, Truong Giang Le**,** Ductile Iron: A Low-Cost Optimal Anode Material for Electrochemical Generation of Ferrate(VI), *Journal of The Electrochemical Society*, **2023**, 170, 8, 83510. (**ISI, Q1**).
2. **Thi Van Anh Nguyen**, Thi Thanh Thuy Mai, Thi Binh Phan, Huu Quang Tran, Minh Quy Bui, Ferrate(VI) green oxidant: electrochemical generation, self-decomposition, and application for reactive red 195 azo dye treatment, *J Chem Technol Biotechno,* **2024,** 99, 2454–2463, **(ISI, Q1).**
3. Thi Thanh Thuy Mai, **Thi Van Anh Nguyen**, Thi Binh Phan, Effect of anode passivation on ferrate(VI) electro-generation using ductile iron anode and application for methylene blue treatment, *Journal of Applied Electrochemistry*, **2024**, 54, 1783–1794. (**ISI, Q2**).
4. **Nguyen Thi Van Anh**, Phan Thi Binh, Mai Thi Xuan, Mai Thi Thanh Thuy, The effect of NaOH concentration on ferrate electrosynthesis, *Vietnam J. Chem*, **2024**, 62, 4, 437-445. (**Scopous, Q3**).
5. **Nguyen Thi Van Anh**, Phan Thi Binh, Tran Huu Quang, Nguyen The Duyen, Phan Hoang Yen, Mai Thi Thanh Thuy, Efficient removal of methyl orange by ferrate(vi), *Vietnam journal of sciences and technology*. (**VAST1, Scopous**, **accepted**)
6. **Nguyễn Thi Vân Anh**, Mai Thị Thanh Thùy, Phan Thị Bình, Nghiên cứu tính chất điện hóa và quá trình tổng hợp ferrate (VI) trên điện cực anot gang xám trong môi trường kiềm đặc, *Tạp chí khoa học và công nghệ Việt Nam*, 2025, 67(9), 6-12.